

Ynamide Protonation-Initiated *Cis*-Selective Polyene Cyclization and Reaction Mechanism

Jiasheng Yao^{1,2†}, Chen-Long Li^{3†}, Xing Fan³, Zhou Wang², Zhi-Xiang Yu^{3*} & Junfeng Zhao^{1,4,5*}

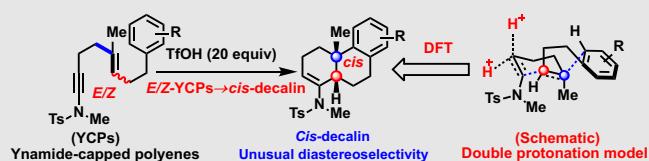
¹School of Pharmaceutical Sciences, Guangzhou Medical University, Guangzhou 511436, ²College of Chemistry and Chemical Engineering, Jiangxi Normal University, Nanchang 330022, ³College of Chemistry, Peking University, Beijing 100871, ⁴School of Chemistry and Chemical Engineering, Northwestern Polytechnical University, Xi'an 710072, ⁵State Key Laboratory of Elemento-Organic Chemistry, Nankai University, Tianjin 300071

*Corresponding authors: yuzx@pku.edu.cn; zhaojf@jxnu.edu.cn; †J. Yao and C.-L. Li contributed equally to this work.

Cite this: *CCS Chem.* **2021**, *3*, 3133–3143

The diastereoselectivity of conventional polyene cyclization reactions is highly dependent on the configuration of the internal alkenes, where *E*-polyenes provide *trans*-decalins, while *Z*-polyenes offer *cis*-decalins. Although polyene cyclization has evolved into a reliable and widely used strategy for the construction of *trans*-decalin frameworks of terpene and steroid natural products, its application for *cis*-decalin framework is extremely challenging. This is because it not only requires the difficultly approached *Z*-polyenes but also has usually been accompanied by the formation of undesired *trans*-isomer. We herein report a universal polyene cyclization approach to *cis*-decalin frameworks by employing ynamide-capped polyenes (YCPs), which erase the traditional strict requirement for alkene stereochemistry since both *E*- and *Z*-YCPs give *cis*-decalin frameworks with excellent diastereoselectivity. A broad range of YCPs are compatible to furnish the *cis*-decalin frameworks in good to excellent yields without any detectable *trans*-isomer. Both experimental and density functional theory

(DFT) calculation results reveal that the ynamide protonation-initiated polyene cyclization proceeds in a stepwise manner involving an unprecedented double protonation mechanism wherein the steric repulsion between the iminium and the forming decalin framework in the Friedel–Crafts transition state is responsible for the unusual excellent *cis*-diastereoselectivity. DFT calculations also showed that an excess of TfOH was essential for the formation of *cis*-decalin because the catalytic amount of TfOH resulted in the pretermination of this cascade process.



Keywords: polyene cyclization, *cis*-decalin framework, ynamide, protonation, double protonation mechanism

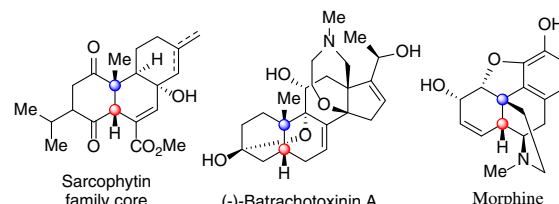
Introduction

Terpenes and steroids containing complex polycyclic frameworks and continuous multiple stereocenters are ubiquitous natural products with intriguing biological

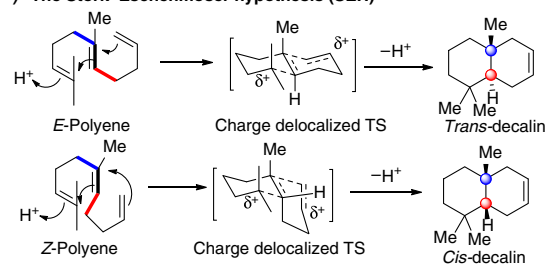
activities.^{1,2} In nature, their polycyclic frameworks are constructed via enzyme-catalyzed protonation-initiated polyene cyclization reactions, wherein up to five C–C bonds and nine continuous stereocenters can be formed with excellent chemo-, regio-, and stereoselectivities.^{3–5} The excellent

efficiency of polyene cyclization reactions has fascinated organic chemists for more than 60 years and inspired investigations of the reaction mechanism and the design of a variety of fantastic biomimetic polyene cyclization reactions in the laboratory.^{6–8} To mimic the polyene cyclization occurring in nature, an isopropenyl group was originally employed as the initiator in the polyene cyclization reactions.^{9–13} In view of the structural diversity of terpenes and steroids as well as the difficulties encountered in the functionalization of the gem-dimethyl group of the final cyclized products, epoxides,¹⁴ aldehydes,¹⁵ vinyl groups,¹⁶ and allylic alcohols,¹⁷ among other functional groups,^{18–20} which can interact with the catalyst or promoter to form a carbenium ion or a radical,^{21–23} have been employed as initiators for polyene cyclization reactions. It is widely believed that the chemo-, regio-, and stereoselectivities of polyene cyclization are governed by the prearranged conformation of the linear precursors. The stereochemistry outcome of polyene cyclizations is predictable according to the Stork–Eschenmoser hypothesis (Scheme 1b),^{24,25} which suggests that polyenes containing *E*-alkene (*E*-polyenes) give *trans*-ring junctions while *Z*-polyenes afford *cis*-ring junctions.²⁶ Owing to these efforts, biomimetic polyene cyclization of *E*-polyenes has evolved into a widely applied and highly reliable strategy for constructing *trans*-decalin frameworks of terpene- and steroid-based natural products and their derivatives.^{8,27–30} However, this strategy has not been applied in the synthesis of *cis*-decalin-containing natural products yet, which are also prevalent in nature (Scheme 1a).^{31–34} This is mainly due to the following two reasons: (1) the preference for the transition state of forming *cis* product over its *trans*-counterpart is marginal for *Z*-polyene substrates, leading to a mixture of *cis*- and *trans*-isomers; (2) synthesizing *Z*-polyene substrates is more difficult than their *E*-polyene counterparts.^{35–38} Only recently has the first polyene cyclization approach to enantioenriched *cis*-decalins from *Z*-polyenes been accomplished by Gleason and co-workers (Scheme 1c, eq 1).³⁹ Interestingly, scattered reports have illustrated that the *cis* ring juncture could be obtained as a side product of some very rare polyene cyclizations of *E*-polyenes albeit with poor selectivity.^{38,40–43} In such a context, we envisioned that a universal approach to *cis*-decalin products from both *E*- and *Z*-polyenes will be much more attractive because the more easily prepared *E*-polyenes rather than the difficultly approached *Z*-polyenes could be used for the challenging *cis*-polyene cyclization (Scheme 1c, eq 2). Another advantage is that the tedious separation of *E*- and *Z*-isomers during the substrate preparation would be unnecessary as the configuration of the alkene in polyenes will not influence the diastereoselectivity. We herein report a universal strategy to solve the long-standing challenge to construct *cis*-decalin frameworks via polyene cyclization of either ynamide-capped *E*-polyenes (*E*-YCPs) or

(a) Natural products containing the *cis*-decalin framework

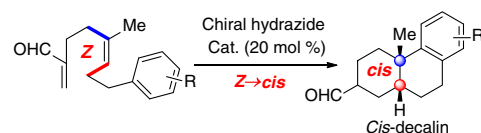


(b) The Stork–Eschenmoser hypothesis (SEH)

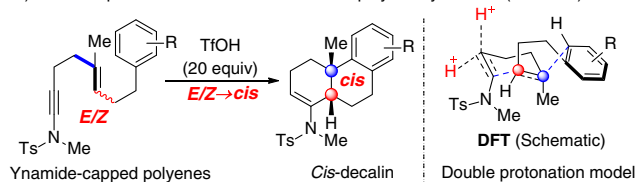


(c) Polyene cyclization approach to *cis*-decalin framework

1) Organocatalyzed polyene cyclization approach to *cis*-decalin



2) Ynamide protonation-initiated *cis*-selective polyene cyclization (this work)



Scheme 1 | (a) Natural products containing *cis*-decalin frameworks, (b) the Stork–Eschenmoser hypothesis, and (c) the polyene cyclization approach to the *cis*-decalin framework.

ynamide-capped *Z*-polyenes (*Z*-YCPs). Additionally, DFT calculations have been conducted, revealing that a unique double protonation mechanism is involved, and the steric repulsion between the iminium and the forming decalin framework in the Friedel–Crafts (F–C) transition state is responsible for the unusual excellent *cis*-diastereoselectivity.

Experimental Methods

General procedure for ynamide protonation-initiated *cis*-selective polyene cyclization

To an oven-dried reaction tube (10 mL) equipped with a magnetic stir bar was added *E*-YCPs **1** (0.1 mmol) in dichloromethane (DCM) (1 mL), and cooled to $-40\text{ }^{\circ}\text{C}$. Then TfOH (2 mmol) was added slowly, and stirred for 10 min. After the reaction was complete, the reaction mixture was treated with saturated aqueous NaHCO_3

solution, extracted with DCM, and the combined organic layers were washed with brine, dried over anhydrous Na_2SO_4 , filtered, and concentrated. The crude extracts were purified by silica gel column chromatography to offer the desired products **2a-2p** and **6a-6m**.

Computational methods

All calculations were performed with the Gaussian 09 program.⁴⁴ Geometry optimizations of all intermediates and transition states were carried out using the hybrid B3LYP^{45,46} functional with the 6-31G(d)⁴⁷ basis set in the gas phase. Frequency calculations at the same level were performed to confirm that each stationary point was either a minimum or a transition state structure and to evaluate its zero-point energy and the thermal corrections at 298 K. To improve their accuracy, single-point energy calculations were carried out using the M06-2X⁴⁸ functional with the 6-311G(d,p)⁴⁷ basis set. Solvation energy ($\Delta G_{\text{solvation}}$) for every species was the computed single-point energy difference in DCM and in the gas phase. Single-point energies in DCM ($\epsilon = 8.93$) were evaluated by SMD⁴⁹ calculations. Gibbs free energies in solutions were obtained from sums of the large basis set gas-phase single-point energies, solvation energies ($\Delta G_{\text{solvation}}$), and the gas-phase Gibbs free energy corrections (at 298 K). The energy profile was drawn according to Gibbs free energies in the DCM solution (ΔG_{sol}). The standard state of 1.0 mol/L at 298 K for all species was used. The computed structures were illustrated using CYLView.⁵⁰

Results and Discussion

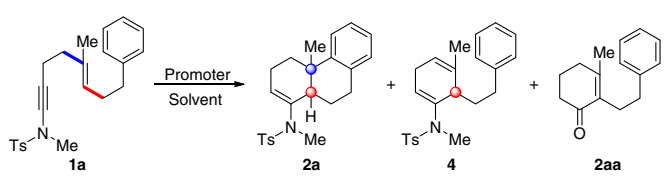
It is well known that the protonation of an ynamide can produce a highly reactive keteniminium ion, which can be used to initiate cationic cascade reactions to construct polycyclic frameworks.⁵¹⁻⁵³ On the other hand, a C-C triple bond has been used as the initiator for polyene cyclization because of its ability to deliver an electrophilic carbon center upon interaction with a carbophilic metal catalyst.⁵⁴⁻⁵⁹ Recently, our group has been interested in both ynamide chemistry⁶⁰⁻⁶⁵ and developing new reactions and strategies for efficient construction of polycyclic compounds.^{66,67} Based on our previous studies, we hypothesized that an ynamide functional group would be a promising initiator for polyene cyclization (Scheme 1c, eq 2). More importantly, the final polycyclic products bearing an extra amino functionality might be highly useful for the synthesis of terpene alkaloids and further manipulation. Preliminary study demonstrated that our proposal was feasible, and the tricyclic decalin **2a** could be obtained as the major product with excellent diastereoselectivity.

Optimization of reaction conditions disclosed that solvent, Brønsted acid promoter and its loading, and reaction temperatures had significant influence on reaction outcomes (Table 1). Generally, less polar solvent favored the

formation of tricyclic product (entries 1, 4, and 5) while more polar nonprotonic solvent favored the generation of monocyclized product (entries 6 and 7). We found that the acidity and loading of the promoter imposed a remarkable effect on the distribution of products. Finally, we were happy to observe that using 20 equiv of triflic acid for the reaction provided the highest chemoselectivity (entries 8-12). In addition, low temperature was beneficial for the formation of the target tricyclic product. The best result was reached when the reaction was carried out in DCM at $-40\text{ }^\circ\text{C}$ with 20 equiv of triflic acid as the promoter (entry 13). Further increasing the loading of the promoter did not offer any improvement (entry 14), but reducing the loading of the promoter favored the formation of monocyclized product (entries 11 and 15). Surprisingly, X-ray crystallography analysis of **2a** illustrated that the relative configuration of the decalin moiety was *cis* rather than the commonly expected *trans* counterpart (Scheme 2, eq 1). This unusual diastereoselectivity motivated us to test the Z-YCP substrate **3**. To our surprise and delight, *cis*-decalin tricyclic product **2a** was still delivered (Scheme 2, eq 2). This result suggested that the present polyene cyclization reaction would proceed in a stepwise manner, in which both *E*- and *Z*-YCP substrates would proceed via the same key intermediate. Fortunately, the preterminated monocyclized product **4** could be obtained as a major product when *E*-YCP **1a** or *Z*-YCP **3** or a mixture of these two substrates was treated with a catalytic amount of triflic acid (20%), (Table 1, entry 15). Compound **4** could be smoothly converted to the final tricyclic product **2a** under the standard cyclization reaction conditions (Scheme 2, eq 3). We therefore proposed that the monocyclized product **4** would be a common intermediate for both the *Z*- and *E*-YCP substrates. Notably, the one-pot two-step protocol afforded the target tricyclic product with similar excellent efficiencies.

With these exciting results in hand, we envisioned that a broad substrate scope for such a reaction would offer a general approach for constructing the challenging *cis*-decalin frameworks from the easily available *E*-YCP substrates. A variety of *E*-YCPs containing aryl terminal groups were prepared and evaluated under the standard cyclization reaction conditions (Scheme 3). In terms of the ynamide moiety, it was revealed that electron-donating substituents on the phenylsulfonamide group of the substrates led to superior results compared to those with electron-withdrawing substituents (i.e., **2a-2e**), and the methylsulfonamide substrate gave a comparable result (**2f**). Substrates bearing both electron-withdrawing and -donating groups on the terminator afforded the target tricyclic products in good to excellent yields (**2g-2l**). In addition, *E*-YCPs with heterocycles as well as aryl substituents on the terminal phenyl ring were also suitable substrates (**2m-2o**). We then explored substrates with halide substituents and found that both chloro- and bromo-substituents were compatible to give the target cyclized products in good yields (**2i**, **2k**).

Table 1 | Reaction Conditions Optimization^a



Entry	Promoter (equiv)	Solvent	T (°C)	Yield (%) ^b		
				2a	4	2aa
1	TfOH (10 equiv)	DCM	0	36	17	—
2	TfOH (10 equiv)	CH ₃ NO ₂	0	27	9	—
3	TfOH (10 equiv)	HFIP	0	37	—	—
4	TfOH (10 equiv)	CHCl ₃	0	37	12	—
5	TfOH (10 equiv)	Toluene	0	39	—	—
6	TfOH (10 equiv)	Acetone	0	—	47	—
7	TfOH (10 equiv)	DMF	0	—	12	—
8	Tf ₂ NH (10 equiv)	DCM	0	13	11	—
9	TFA (10 equiv)	DCM	0	8	20	—
10	MsOH (10 equiv)	DCM	0	8	—	53
11	TfOH (5 equiv)	DCM	0	13	31	—
12	TfOH (20 equiv)	DCM	0	62	—	—
13	TfOH (20 equiv)	DCM	-40	90	—	—
14	TfOH (40 equiv)	DCM	-40	91	—	—
15	TfOH (0.2 equiv)	DCM	-40	—	77	—

Note: DMF, dimethylformamide; HFIP, hexafluoroisopropanol; TFA, trifluoroacetic acid. Bold format is used to highlight that entry 13 is the best reaction condition.

^a Reaction conditions: **1a** (0.05 mmol), solvent (1 mL).

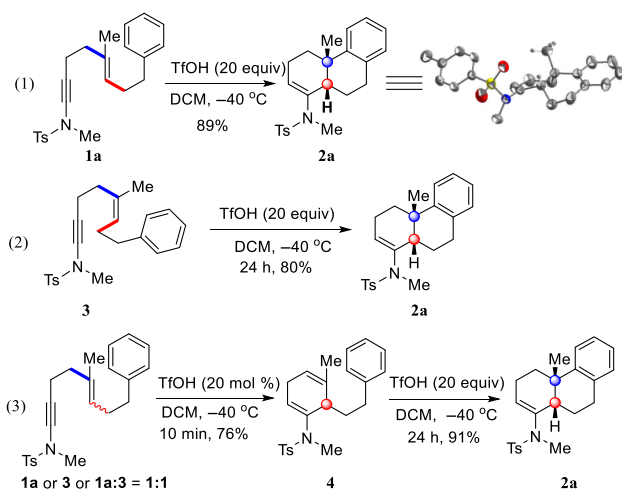
^b Measured by using crude ¹H NMR with 3,4,5-trimethoxyphenyl as the internal standard.

We noted that both *para*- and *ortho*-cyclized products (**2i**, **2i'**) were formed in yields of 47% and 26%, respectively, when *m*-Br-Ph- was employed as the terminator. The compatibility of the halide substituents in such a polyene cyclization reaction offered opportunities for further functionalization via transition metal catalyzed cross-coupling reactions using these halide-containing

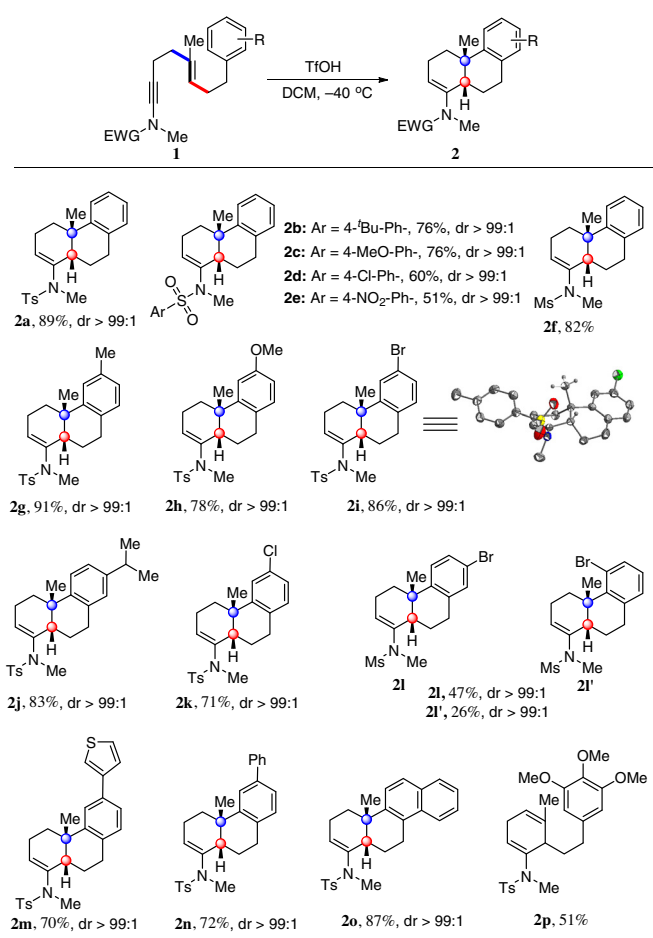
products, greatly expanding the impact of this method in synthesis. Unfortunately, only monocyclized product **2p** was obtained in 51% yield when a 3,4,5-trimethoxyphenyl group was employed as the terminator in the reaction.

To further illustrate the generality of this method, the polyene cyclization was investigated by using substrates containing ether linkages. As shown in Scheme 4, oxygen-containing *E*-YCP substrates could be transformed to the *cis*-decalin ring systems with excellent chemo-, stereo-, and regioselectivities. The structures of the tricyclic products **6c** and **6i** were unambiguously confirmed by NMR and X-ray crystallography. Similarly, both electron-withdrawing and -donating groups on the terminal phenyl ring in the substrates were compatible in the reaction (**6b–6k**); however, the preterminated monocyclized products **6l** and **6m** were obtained when the strong electron-withdrawing group of -NO₂ or two electron-donating -OMe groups were present on the terminal phenyl ring of the substrates. Moreover, the target tricyclic product **6k** and its deprotected product **6k'** were both obtained in 39% and 36% yields, respectively, for the substrate with a benzyloxy group on its aryl terminal group.

To study the synthetic application of this methodology, further transformations of the polycyclic products were



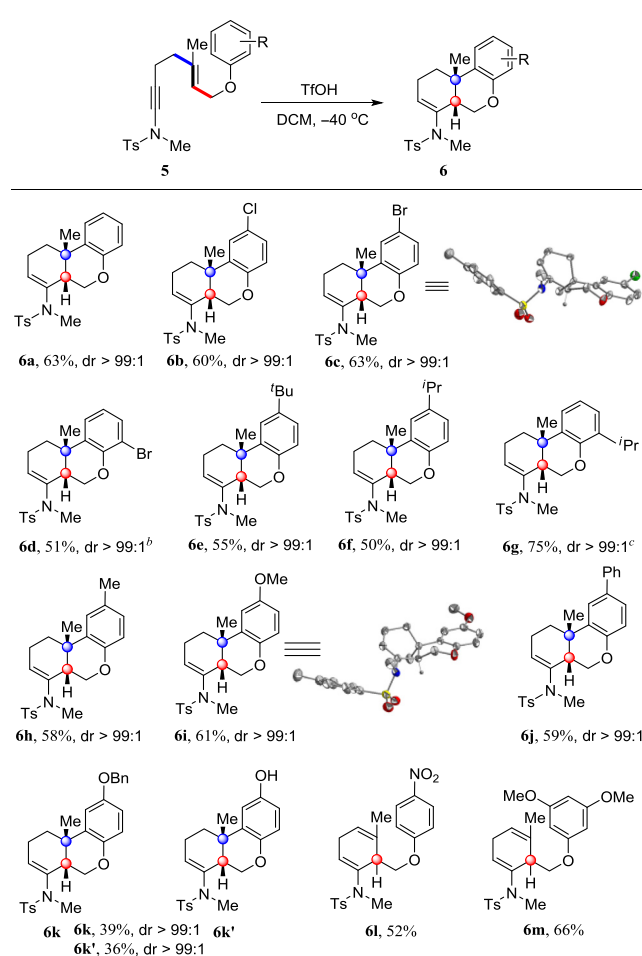
Scheme 2 | Discovery of *cis*-selective polyene cyclization.



Scheme 3 | Substrate scope of the unusual polyene cyclization. ^aReaction conditions: **1** (0.1 mmol), TfOH (2 mmol), DCM (1 mL), -40 °C, 10 min.

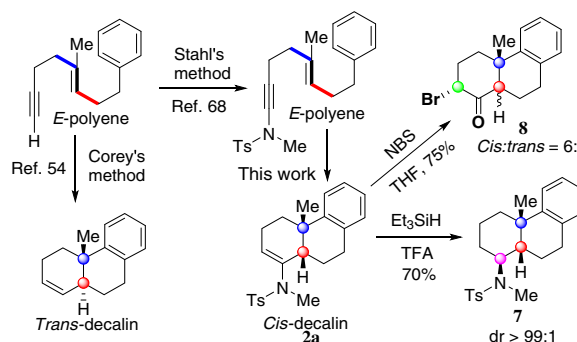
conducted (Scheme 5). For example, the enamide double bond of *cis*-decalin **2a** could be reduced smoothly to furnish **7**, which is an attractive intermediate for terpene alkaloid synthesis, with excellent diastereoselectivity (dr > 99:1). In addition, we observed that the α -bromoketone **8**, in which the bromo and ketone functional groups offer tags for further functionalization, could be obtained in a good yield and diastereoselectivity by treating **2a** with *N*-bromosuccinimide. Notably, the *E*-YCPs could be easily prepared from Corey's terminal alkynyl *E*-polyenes, which afforded the *trans*-decalin framework upon treatment with In(III) reagent,⁵⁴ via an oxidative cross-coupling reaction.⁶⁸ This means that both *trans*- and *cis*-decalin frameworks are approachable from the same terminal alkynyl *E*-polyene substrates by employing Corey's method⁵⁴ directly (Scheme 5, left part) or by capping the terminal alkyne group with ynamide followed by the polyene cyclization of *E*-YCPs (Scheme 5, middle part).

DFT calculations were carried out to understand the unusual *cis*-diastereoselectivity of the ynamide protonation-initiated polyene cyclization. A plausible reaction

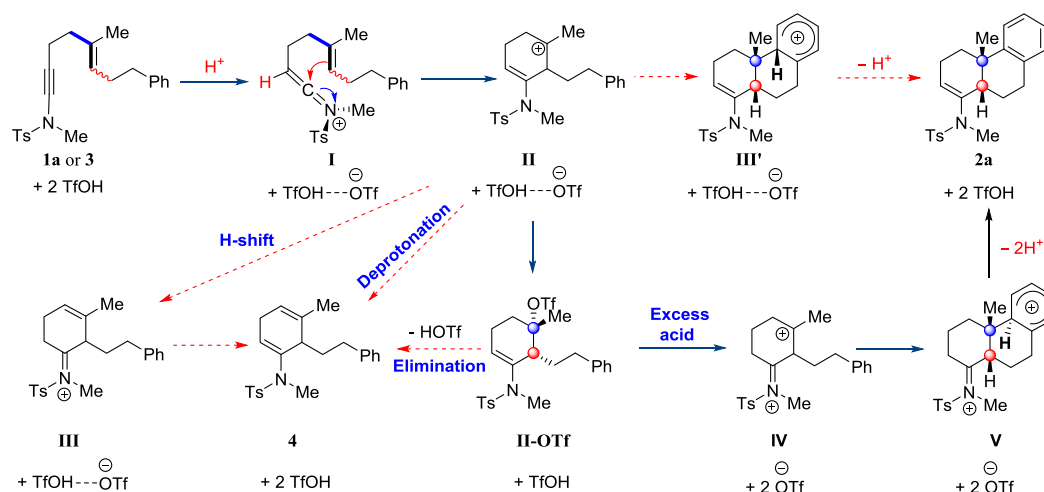


Scheme 4 | Substrate scope of the oxygen-containing *E*-YCPs. ^aReaction conditions: **5** (0.1 mmol), TfOH (2 mmol), DCM (1 mL), -40 °C, 24 h. ^bTfOH (3 mmol), DCM (1 mL), -20 °C, 2 d. ^cTfOH (3 mmol), DCM (1 mL), -40 °C, 4 d.

mechanism, which was also supported by DFT calculations, was proposed in Scheme 6. Protonation of the *E*-YCP (**1a**) or *Z*-YCP (**3**) by one TfOH molecule (two TfOH molecules were used to mimic the presence of a cluster of TfOH molecules in the reaction system in our calculations)



Scheme 5 | Synthetic application of the cyclized product.



Scheme 6 | Proposed reaction mechanism.

gave the highly reactive keteniminium ion **I**, which then underwent electrophilic addition toward the alkene, giving the carbenium ion **II**. Then this intermediate, via cyclization, afforded **III'**. This step was followed by deprotonation, delivering *cis*-product **2a** (the formation of *trans*-product from this step was disfavored compared to that of *cis*-product, see the Supporting Information Scheme S2). However, this pathway was disfavored because there was another competing and much more favored pathway in which intermediate **II** could easily be trapped by the OTf anion in the TfOH cluster, forming intermediate **II-OTf**. This species was then transformed to compound **4** via elimination. Actually **4** was observed when a catalytic amount of TfOH was used (Table 1, entry 15 and Scheme 2, eq 2), giving experimental support to this proposal.

When excess triflic acid was used, compound **1a** or **3** still gave **II-OTf** by the same processes. But **II-OTf** then underwent further protonation to give a dicationic intermediate, **IV** (via protonation of the OTf group, a barrierless C-O dissociation process to lose a TfOH molecule, and then protonation of the enamine moiety, see Supporting Information Scheme S5), which then underwent F-C alkylation with the aryl ring and deprotonation followed to afford the final tricyclic product **2a**. When *Z*-polyene **3** was used as the substrate, it experienced the same double protonation processes to give **IV** and the final tricyclic product **2a**.

DFT calculations were performed to explain why dication **IV** favored giving *cis*-product (Figures 1a and 1b). We started our calculations from the intermediate **I**, which was generated by an exergonic protonation of substrate **1a** or **3**. The cyclization was easy with an activation free energy of 0.5 kcal/mol. This step gave cationic intermediate **II**. Theoretically, **II** can undergo cyclization to give the *cis*-product **2a**, which only requires an activation free energy of 2.4 kcal/mol (*trans*-product formation is not

favored, see the Supporting Information Scheme S2). Therefore, these calculations imply that cyclization from **II** is faster than a diffusion process and cannot be intercepted by another reagent, if the above proposal is correct. But TfOH was used in 20%, and a cluster of TfOH molecules was formed in the solvent, suggesting that intermediate **II** was actually surrounded by TfOH-OTf anion. This implies that once intermediate **II** is formed, it can be quickly quenched by its adjacent OTf anion to form **II-OTf**. This neutral intermediate then underwent an elimination reaction to form **4**, with a computed activation free energy of 20.3 kcal/mol. Although **II-OTf** is more stable than **4** by 8.2 kcal/mol in terms of free energy, **4** can still be generated considering the quick consumption of generated TfOH by **1a** (see Supporting Information Scheme S1). Moreover, the direct formation of **4** via deprotonation by OTf anion from **II** is a barrierless process, although this is less feasible because intermediate **II-OTf** is more stable (see the Supporting Information Schemes S3 and S4).

When TfOH was used in excess amounts, both the OTf group and the enamine moieties in **II-OTf** were protonated, followed by liberation of a TfOH molecule to afford the dicationic intermediate **IV** (see the Supporting Information Schemes S5-S7). Two electrophilic transition states, starting from **IV**, leading to *cis*- and *trans*-products, respectively, were located. We found that the dication in the *cis*-pathway via **TS-IV-V**, required only an activation free energy of 1.1 kcal/mol to give **V**, which then furnished the *cis*-product by deprotonation. In contrast, two steps were required in the *trans*-pathway. DFT calculations showed that a bicyclic cation intermediate **VI** was firstly generated from **IV** via **TS-IV-VI** with an activation free energy of 13.7 kcal/mol. This step was endergonic by 6.5 kcal/mol. Secondly, an easy C-C bond migration via **TS-VI-VII**, with an activation free energy of only 6.5 kcal/mol, took place to give a more stable intermediate **VII**. The DFT results in Figure 1b clearly show that *trans*-product will not be

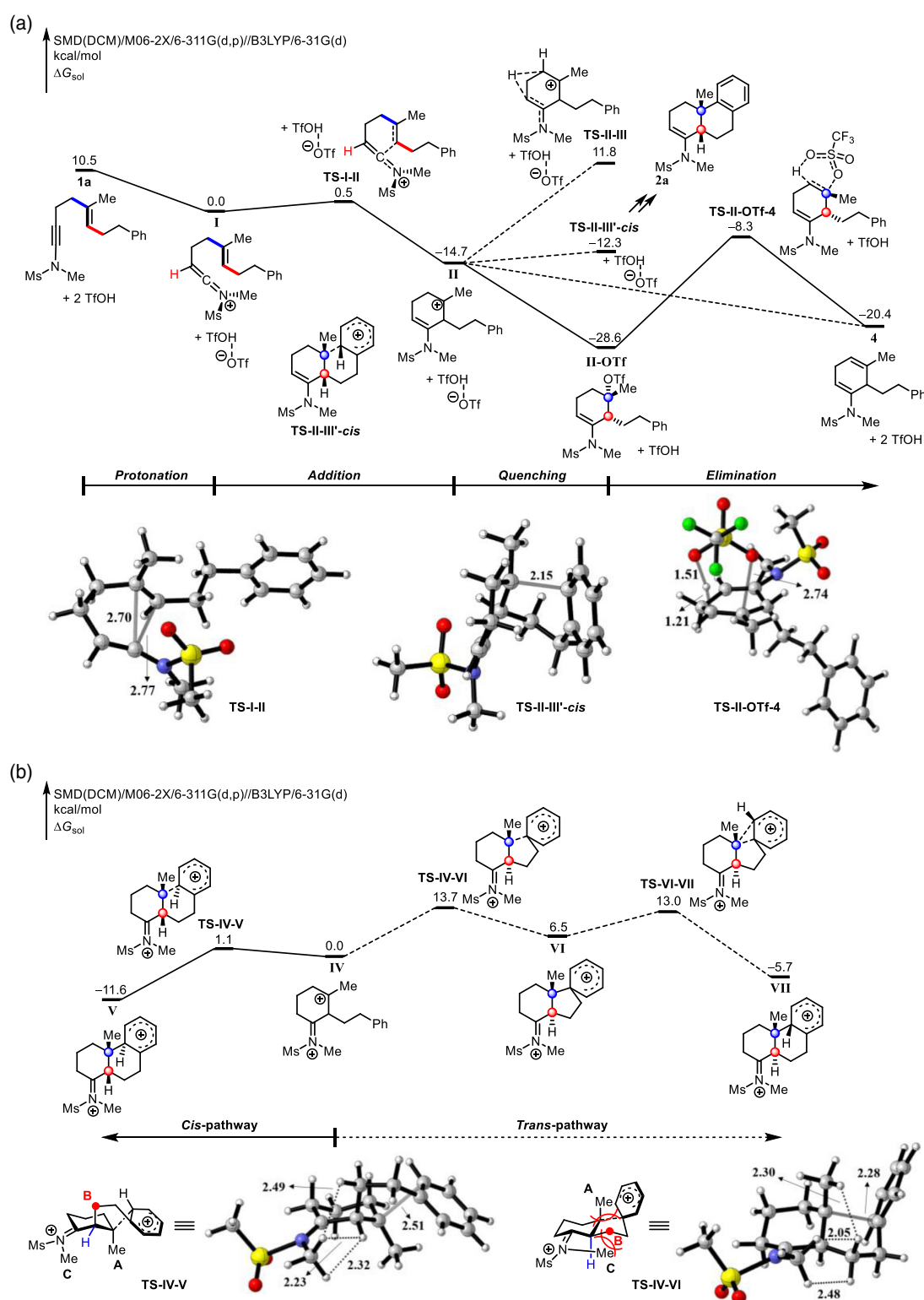


Figure 1 | (a) DFT-computed energy surface for the generation of **4** and (b) DFT-computed energy surface for the formation of *cis*- and *trans*-products (bond distances in angstrom).

formed because this pathway needs an activation free energy of 13.7 kcal/mol, which is 12.6 kcal/mol less favored than that required in the *cis*-pathway. The final step of

deprotonation from **V** and **VII** is expected to be quite easy, as suggested by our calculations of deprotonation by OTf anion (see the [Supporting Information Scheme S8](#)).

Therefore, DFT calculations suggest that the *trans*-product will not be generated kinetically, in agreement with the experimental results.

Two steric hindrances can be invoked to explain the *cis*-selectivity. It was firstly found that the iminium's methyl group showed a strong 1,3-repulsion with the equatorial alkyl group in the **TS-IV-VI** (groups B and C in Figure 1b, the distance between methyl hydrogen and methylene hydrogen is only 2.05 Å). The second hindrance could arise from the repulsion of groups A and B in **TS-IV-VI**, in which the distance of two hydrogen atoms is 2.30 Å. However, the steric repulsions cannot be found in the *cis*-decalin formation transition state, in which A and B groups are in a *trans*-configuration, and A and C groups are in a stagger conformation. These two factors lead to the result that *trans*-transition state **TS-IV-VI** is greatly disfavored compared to the *cis*-transition state **TS-IV-V** by 12.6 kcal/mol. A schematic picture to rationalize the unusual *cis*-diastereoselectivity of the ynamide protonation-initiated polyene cyclization is given in Scheme 1c, where double (but stepwise) protonation and F-C reaction are shown together to have a quick and easy understanding of the whole process. Experimentally, it was observed that substrate **5l** bearing a NO₂ group failed to furnish the final tricyclic product, and this could be attributed to the slower F-C reaction of the NO₂-substituted aryl ring in the substrate. For substrates **1p** and **5m** containing three or two methoxyl groups, poor experimental results could be explained by protonation of the OMe group by strong acid which deactivated the aryl ring for the F-C reaction.

Conclusion

We have successfully developed a general synthetic approach to *cis*-decalin frameworks via an unprecedented ynamide protonation-initiated polyene cyclization by using ynamide-capped polyenes (YCPs). Unlike the conventional polyene cyclization reactions wherein *E*-polyenes lead to *trans*-decalins while *Z*-polyenes offer *cis*-decalins, both *E*- and *Z*-YCPs furnish the *cis*-decalin frameworks with excellent chemo-, regio-, and diastereoselectivities in the present cyclization reaction, and thus providing an easy and general way to build *cis*-decalin frameworks, a long-standing challenge in the polyene cyclization field. Considering the fact that the ynamide-capped polyene substrates (YCPs) could be easily prepared from Corey's *E*-polyene substrates, which afford the *trans*-decalines by the traditional method, present method possessed an additional advantage that it made the *cis*- as well as *trans*-decalin frameworks approachable from the same readily available Corey's *E*-polyene substrates. DFT study indicated that this ynamide protonation-initiated polyene

cyclization proceeded via a double protonation pathway through the keteniminium ion and iminium dications, respectively. The DFT calculations disclosed that the steric repulsions between the iminium and the forming decalin framework in the F-C transition state play a crucial role in determining the unusual *cis*-diastereoselectivity. Considering the diversity of polycyclic frameworks in natural products and pharmaceuticals, novel reactions and strategies for efficiently constructing polycyclic frameworks are highly demanded. The present method, together with our previous gold catalyzed dienediyne polycyclization,^{69,70} represents our ongoing efforts in this field.⁷¹

Supporting Information

Supporting Information is available including experimental details and characterization, computational results and discussions.

Conflict of Interest

The authors declare no competing financial interest.

Acknowledgments

This work was supported by the National Natural Science Foundation of China (nos. 21778025, 91853114, and 2193303) and the Natural Science Foundation of Jiangxi Province (no. 20202ACBL203004). We dedicate this work to the 100th anniversary of chemistry at Nankai University.

References

1. Tietze, L. F. Domino Reactions in Organic Synthesis. *Chem. Rev.* **1996**, *96*, 115–136.
2. Poupon, E.; Nay, B. *Biomimetic Organic Synthesis*; Wiley-VCH: Weinheim, **2011**.
3. de la Torre, M. C.; Sierra, M. A. Comments on Recent Achievements in Biomimetic Organic Synthesis. *Angew. Chem. Int. Ed.* **2004**, *43*, 160–181.
4. Thoma, R.; Schulz-Gasch, T.; D'Arcy, B.; Benz, J.; Aebi, J.; Dehmlow, H.; Hennig, M.; Stihle, M.; Ruf, A. Insight into Steroid Scaffold Formation from the Structure of Human Oxidosqualene Cyclase. *Nature* **2004**, *432*, 118–122.
5. Wendt, K. U.; Schulz, G. E.; Corey, E. J.; Liu, D. R. Enzyme Mechanisms for Polycyclic Triterpene Formation. *Angew. Chem. Int. Ed.* **2000**, *39*, 2812–2833.
6. Yoder, R. A.; Johnston, J. N. A Case Study in Biomimetic Total Synthesis: Polyolefin Carbocyclizations to Terpenes and Steroids. *Chem. Rev.* **2005**, *105*, 4730–4756.
7. Ungarean, C. N.; Southgate, E. H.; Sarlah, D. Enantioselective Polyene Cyclizations. *Org. Biomol. Chem.* **2016**, *14*, 5454–5467.

8. Barrett, A. G. M.; Ma, T.-K.; Mies, T. Recent Developments in Polyene Cyclizations and Their Applications in Natural Product Synthesis. *Synthesis* **2019**, *51*, 67–82.
9. Ishihara, K.; Nakamura, S.; Yamamoto, H. The First Enantioselective Biomimetic Cyclization of Polyprenoids. *J. Am. Chem. Soc.* **1999**, *121*, 4906–4907.
10. Sakakura, A.; Ukai, A.; Ishihara, K. Enantioselective Halocyclization of Polyprenoids Induced by Nucleophilic Phosphoramidites. *Nature* **2007**, *445*, 900–903.
11. Samanta, R. C.; Yamamoto, H. Catalytic Asymmetric Bromocyclization of Polyenes. *J. Am. Chem. Soc.* **2017**, *139*, 1460–1463.
12. Zhao, Y.-J.; Chng, S.-S.; Loh, T.-P. Lewis Acid-Promoted Intermolecular Acetal-Initiated Cationic Polyene Cyclizations. *J. Am. Chem. Soc.* **2007**, *129*, 492–493.
13. Tao, Z.; Robb, K. A.; Zhao, K.; Denmark, S. E. Enantioselective, Lewis Base-Catalyzed Sulfenocyclization of Polyenes. *J. Am. Chem. Soc.* **2018**, *140*, 3569–3573.
14. Corey, E. J.; Cheng, H.; Baker, C. H.; Matsuda, S. P. T.; Li, D.; Song, X. Studies on the Substrate Binding Segments and Catalytic Action of Lanosterol Synthase. Affinity Labeling with Carbocations Derived from Mechanism-Based Analogs of 2,3-Oxidosqualene and Site-Directed Mutagenesis Probes. *J. Am. Chem. Soc.* **1997**, *119*, 1289–1296.
15. Zhu, L.; Luo, J.; Hong, R. Total Synthesis of (\pm)-Cafestol: A Late-Stage Construction of the Furan Ring Inspired by a Biosynthesis Strategy. *Org. Lett.* **2014**, *16*, 2162–2165.
16. Mullen, C. A.; Campbell, A. N.; Gagne, M. R. Asymmetric Oxidative Cation/Olefin Cyclization of Polyenes: Evidence for Reversible Cascade Cyclization. *Angew. Chem. Int. Ed.* **2008**, *47*, 6011–6014.
17. Schafroth, M. A.; Sarlah, D.; Krautwald, S.; Carreira, E. M. Iridium-Catalyzed Enantioselective Polyene Cyclization. *J. Am. Chem. Soc.* **2012**, *134*, 20276–20278.
18. Bender, J. A.; Arif, A. M.; West, F. G. Nazarov-Initiated Diastereoselective Cascade Polycyclization of Aryltrienones. *J. Am. Chem. Soc.* **1999**, *121*, 7443–7444.
19. Zhao, Y.-J.; Li, B.; Tan, L.-J. S.; Shen, Z.-L.; Loh, T.-P. Enantioselective Cationic Polyene Cyclization vs Enantioselective Intramolecular Carbonyl-Ene Reaction. *J. Am. Chem. Soc.* **2010**, *132*, 10242–10244.
20. Knowles, R. R.; Lin, S.; Jacobsen, E. N. Enantioselective Thiourea-Catalyzed Cationic Polycyclizations. *J. Am. Chem. Soc.* **2010**, *132*, 5030–5032.
21. Heinemann, C.; Demuth, M. Biomimetic Cascade Cyclizations of Terpenoid Polyalkenes via Photoinduced Electron Transfer. Long-Distance Asymmetric Induction by a Chiral Auxiliary. *J. Am. Chem. Soc.* **1997**, *119*, 1129–1130.
22. Yang, D.; Ye, X. Y.; Gu, S.; Xu, M. Lanthanide Triflates Catalyze Mn(III)-Based Oxidative Radical Cyclization Reactions. Enantioselective Synthesis of (-)-Triptolide, (-)-Triptonide, and (+)-Triptophenolide. *J. Am. Chem. Soc.* **1999**, *121*, 5579–5580.
23. Rendler, S.; MacMillan, D. W. C. Enantioselective Polyene Cyclization via Organo-SOMO Catalysis. *J. Am. Chem. Soc.* **2010**, *132*, 5027–5028.
24. Stork, G.; Burgstahler, A. W. The Stereochemistry of Polyene Cyclization. *J. Am. Chem. Soc.* **1955**, *77*, 5068–5077.
25. Eschenmoser, A.; Ruzicka, L.; Jeger, O.; Arigoni, D. Zur Kenntnis der Triterpene. 190. Mitteilung. Eine Stereochemische Interpretation der Biogenetischen Isoprenregel bei den Triterpenen. *Helv. Chim. Acta* **1955**, *38*, 1890–1904.
26. Eschenmoser, A.; Arigoni, D. Revisited after 50 Years: The ‘Stereochemical Interpretation of the Biogenetic Isoprene Rule for the Triterpenes’. *Helv. Chim. Acta* **2005**, *88*, 3011–3050.
27. Jeker, O. F.; Kravina, A. G.; Carreira, E. M. Total Synthesis of (+)-Asperolide C by Iridium-Catalyzed Enantioselective Polyene Cyclization. *Angew. Chem. Int. Ed.* **2013**, *52*, 12166–12169.
28. Hong, B.; Liu, W.; Wang, J.; Wu, J.; Kadonaga, Y.; Cai, P.-J.; Lou, H.-X.; Yu, Z.-X.; Li, H.; Lei, X. Photoinduced Skeletal Rearrangements Reveal Radical-Mediated Synthesis of Terpenoids. *Chem* **2019**, *5*, 1671–1681.
29. Zhou, S.; Guo, R.; Yang, P.; Li, A. Total Synthesis of Septedine and 7-Deoxyseptedine. *J. Am. Chem. Soc.* **2018**, *140*, 9025–9029.
30. Cherney, E. C.; Green, J. C.; Baran, P. S. Synthesis of ent-Kaurane and Beyerane Diterpenoids by Controlled Fragmentations of Overbred Intermediates. *Angew. Chem. Int. Ed.* **2013**, *52*, 9019–9022.
31. Guo, Y.; Guo, Z.; Lu, J.-T.; Fang, R.; Chen, S.-C.; Luo, T. Total Synthesis of (-)-Batrachotoxinin A: A Local-Desymmetrization Approach. *J. Am. Chem. Soc.* **2020**, *142*, 3675–3679.
32. Nannini, L. J.; Nemat, S. J.; Carreira, E. M. Total Synthesis of (+)-Sarcophytin. *Angew. Chem. Int. Ed.* **2018**, *57*, 823–826.
33. Zhang, Q.; Zhang, F.-M.; Zhang, C.-S.; Liu, S.-Z.; Tu, Y.-Q. Enantioselective Synthesis of Cis-Hydrobenzofurans Bearing All-Carbon Quaternary Stereocenters and Application to Total Synthesis of (-)-Morphine. *Nat. Commun.* **2019**, *10*, 2507.
34. Chen, P.; Wang, C.; Yang, R.; Xu, H.; Wu, J.; Jiang, H.; Chen, K.; Ma, Z. Asymmetric Total Synthesis of Dankasterones A and B and Periconiastone A through Radical Cyclization. *Angew. Chem. Int. Ed.* **2021**, *60*, 5512–5518.
35. Godeau, J.; Fontaine-Vive, F.; Antoniotti, S.; Duñach, E. Experimental and Theoretical Studies on the Bismuth-Triflate-Catalysed Cycloisomerisation of 1,6,10-Trienes and Aryl Polyenes. *Chem. Eur. J.* **2012**, *18*, 16815–16822.
36. Van der Gen, A.; Wiedhaup, K.; Swoboda, J.; Dunathan, H. C.; Johnson, W. S. Nonenzymic Biogenetic-like Olefinic Cyclizations. Stereospecific Cyclization of Dienic Acetals. *J. Am. Chem. Soc.* **1973**, *95*, 2656–2663.
37. Dijkink, J.; Speckamp, W. N. Biomimetic Heterocyclisation of Aryl Olefins One-Step Formation of Two Carbon-Carbon Bonds. *Tetrahedron* **1978**, *34*, 173–178.
38. Snowden, R. L.; Eichenberger, J. C.; Linder, S. M.; Sonnay, P.; Vial, C.; Schulte-Elte, K. H. Internal Nucleophilic Termination in Biomimetic Acid Mediated Polyene Cyclizations: Stereochemical and Mechanistic Implications. Synthesis of (\pm)-Ambrox and Its Diastereoisomers. *J. Org. Chem.* **1992**, *57*, 955–960.
39. Plamondon, S. J.; Warnica, J. M.; Kaldre, D.; Gleason, J. L. Hydrazide-Catalyzed Polyene Cyclization: Asymmetric Organocatalytic Synthesis of Cis-Decalins. *Angew. Chem. Int. Ed.* **2020**, *59*, 253–258.

40. Imagawa, H.; Iyemaga, T.; Nishizawa, M. Mercuric Triflate-Catalyzed Tandem Cyclization Leading to Polycarbocycles. *Org. Lett.* **2005**, *7*, 451–453.
41. Murata, S.; Suzuki, T. Cyclization of Terpene Alcohols and Related Polyenols by Benzeneselenenyl Triflate. *Tetrahedron Lett.* **1990**, *31*, 6535–6538.
42. Feducia, J. A.; Gagne, M. R. Reversibility Effects on the Stereoselectivity of Pt(II)-Mediated Cascade Poly-ene Cyclizations. *J. Am. Chem. Soc.* **2008**, *130*, 592–599.
43. Johnson, W. S.; Crandall, J. K. Olefinic Cyclizations. VII. Formolysis of Cis- and Trans-5,9-Decadienyl p-Nitrobenzenesulfonate and of Some Isomeric Monocyclic Esters. *J. Org. Chem.* **1965**, *30*, 1785–1790.
44. Frisch, M. J.; Trucks, G. W.; Schlegel, H. B.; Scuseria, G. E.; Robb, M. A.; Cheeseman, J. R.; Scalmani, G.; Barone, V.; Mennucci, B.; Petersson, G. A.; Nakatsuji, H.; Caricato, M.; Li, X.; Hratchian, H. P.; Izmaylov, A. F.; Bloino, J.; Zheng, G.; Sonnenberg, J. L.; Hada, M.; Ehara, M.; Toyota, M.; Fukuda, R.; Hasegawa, J.; Ishida, M.; Nakajima, T.; Honda, Y.; Kitao, O.; Nakai, H.; Vreven, T.; Montgomery, J. A., Jr.; Peralta, J. E.; Ogliaro, F.; Bearpark, M.; Heyd, J. J.; Brothers, E.; Kudin, K. N.; Staroverov, V. N.; Keith, T.; Kobayashi, R.; Normand, J.; Raghavachari, K.; Rendell, A.; Burant, J. C.; Iyengar, S. S.; Tomasi, J.; Cossi, M.; Rega, N.; Millam, J. M.; Klene, M.; Knox, J. E.; Cross, J. B.; Bakken, V.; Adamo, C.; Jaramillo, J.; Gomperts, R.; Stratmann, R. E.; Yazyev, O.; Austin, A. J.; Cammi, R.; Pomelli, C.; Ochterski, J. W.; Martin, R. L.; Morokuma, K.; Zakrzewski, V. G.; Voth, G. A.; Salvador, P.; Dannenberg, J. J.; Dapprich, S.; Daniels, A. D.; Farkas, O.; Foresman, J. B.; Ortiz, J. V.; Cioslowski, J.; Fox, D. J. *Gaussian 09*, Revision E.01; Gaussian, Inc.: Wallingford, CT, **2013**.
45. Becke, A. D. Density-Functional Thermochemistry. III. The Role of Exact Exchange. *J. Chem. Phys.* **1993**, *98*, 5648–5652.
46. Lee, C.; Yang, W.; Parr, R. G. Development of the Colle-Salvetti Correlation-Energy Formula into a Functional of the Electron Density. *Phys. Rev. B* **1988**, *37*, 785–789.
47. Hehre, W. J.; Radom, L.; Schleyer, P. v. R.; Pople, J. A. *Ab Initio Molecular Orbital Theory*; Wiley: New York, **1986**.
48. Zhao, Y.; Truhlar, D. G. The M06 Suite of Density Functionals for Main Group Thermochemistry, Thermochemical Kinetics, Noncovalent Interactions, Excited States, and Transition Elements: Two New Functionals and Systematic Testing of four M06-Class Functionals and 12 Other Functionals. *Theor. Chem. Acc.* **2008**, *120*, 215–241.
49. Marenich, A. V.; Cramer, C. J.; Truhlar, D. G. Universal Solvation Model Based on Solute Electron Density and on a Continuum Model of the Solvent Defined by the Bulk Dielectric Constant and Atomic Surface Tensions. *J. Phys. Chem. B* **2009**, *113*, 6378–6396.
50. Legault, C. Y. *CYLVIEW*, 1.0b; Université de Sherbrooke, **2009**. <http://www.cylview.org> (accessed Oct. 17, 2020).
51. DeKorver, K. A.; Wang, X.-N.; Walton, M. C.; Hsung, R. P. Carbocyclization Cascades of Allyl Ketenimines via Aza-Claisen Rearrangements of N-Phosphoryl-N-allyl-yenamides. *Org. Lett.* **2012**, *14*, 1768–1771.
52. Zhang, Y.; Hsung, R. P.; Zhang, X.; Huang, J.; Slafer, B. W.; Davis, A. Brønsted Acid-Catalyzed Highly Stereoselective Arene-Ynamide Cyclizations. A Novel Keteniminium Pictet-Spengler Cyclization in Total Syntheses of (±)-Desbro-moarborescines A and C. *Org. Lett.* **2005**, *7*, 1047–1050.
53. Theunissen, C.; Métayer, B.; Henry, N.; Compain, G.; Marrot, J.; Martin-Mingot, A.; Thibaudeau, S.; Evano, G. Keteniminium Ion-Initiated Cascade Cationic Polycyclization. *J. Am. Chem. Soc.* **2014**, *136*, 12528–12531.
54. Surendra, K.; Corey, E. J. Diiodoindium(III) Cation, InI_2^+ , a Potent Yneophile. Generation and Application to Cationic Cyclization by Selective π -Activation of $\text{C}\equiv\text{C}$. *J. Am. Chem. Soc.* **2014**, *136*, 10918–10920.
55. Qiu, W.-W.; Surendra, K.; Yin, L.; Corey, E. J. Selective Formation of Six-Membered Oxa- and Carbocycles by the In(III)-Activated Ring Closure of Acetylenic Substrates. *Org. Lett.* **2011**, *13*, 5893–5895.
56. Fürstner, A.; Morency, L. On the Nature of the Reactive Intermediates in Gold-Catalyzed Cycloisomerization Reactions. *Angew. Chem. Int. Ed.* **2008**, *47*, 5030–5033.
57. Toullec, P. Y.; Blarre, T.; Michelet, V. Mimicking Polyolefin Carbocyclization Reactions: Gold-Catalyzed Intramolecular Phenoxy cyclization of 1,5-Enynes. *Org. Lett.* **2009**, *11*, 2888–2891.
58. Sethofer, S. G.; Mayer, T.; Toste, F. D. Gold(I)-Catalyzed Enantioselective Polycyclization Reactions. *J. Am. Chem. Soc.* **2010**, *132*, 8276–8277.
59. Rong, Z.; Echavarren, A. M. Broad Scope Gold(I)-Catalyzed Polyenyne Cyclisations for the Formation of Up to Four Carbon-Carbon Bonds. *Org. Biomol. Chem.* **2017**, *15*, 2163–2167.
60. Hu, L.; Xu, S.; Zhao, Z.; Yang, Y.; Peng, Z.; Yang, M.; Wang, C.; Zhao, J. Ynamides as Racemization-Free Coupling Reagents for Amide and Peptide Synthesis. *J. Am. Chem. Soc.* **2016**, *138*, 13135–13138.
61. Yang, J.; Wang, C.; Xu, S.; Zhao, J. Ynamide-Mediated Thiopeptide Synthesis. *Angew. Chem. Int. Ed.* **2019**, *58*, 1382–1386.
62. Tu, Y.; Zeng, X.; Wang, H.; Zhao, J. A Robust One-Step Approach to Ynamides. *Org. Lett.* **2018**, *20*, 280–283.
63. Peng, Z.; Zhang, Z.; Tu, Y.; Zeng, X.; Zhao, J. Regio- and Stereo-Selective Intermolecular Hydroamidation of Ynamides: An Approach to (Z)-Ethene-1,2-Diamides. *Org. Lett.* **2018**, *20*, 5688–5691.
64. Yang, M.; Wang, X.; Zhao, J. Ynamide-Mediated Macrolactonization. *ACS Catal.* **2020**, *10*, 5230–5235.
65. Liu, T.; Xu, S.; Zhao, J. Recent Advances in Ynamide Coupling Reagent. *Chin. J. Org. Chem.* **2021**, *41*, 873–887.
66. Fan, L.; Han, C.; Li, X.; Yao, J.; Wang, Z.; Yao, C.; Chen, W.; Wang, T.; Zhao, J. Enantioselective Polyene Cyclization Catalyzed by a Chiral Brønsted Acid. *Angew. Chem. Int. Ed.* **2018**, *57*, 2115–2119.
67. Wang, K.; Jiang, C.; Zhang, Z.; Han, C.; Wang, X.; Li, Y.; Chen, K.; Zhao, J. Cut and Sew: Benzofuran-Ring-Opening Enabled Cyclopentenone Ring Formation. *Chem. Commun.* **2020**, *56*, 12817–12820.

68. Hamada, T.; Ye, X.; Stahl, S. S. Copper-Catalyzed Aerobic Oxidative Amidation of Terminal Alkynes: Efficient Synthesis of Ynamides. *J. Am. Chem. Soc.* **2008**, *130*, 833–835.
69. Cai, P.-J.; Wang, Y.; Liu, C.-H.; Yu, Z.-X. Gold(I)-Catalyzed Polycyclization of Linear Dienenynes to Seven-Membered Ring-Containing Polycycles via Tandem Cyclopropanation/Cope Rearrangement/C-H Activation. *Org. Lett.* **2014**, *16*, 5898–5901.
70. Wang, Y.; Cai, P.-J.; Yu, Z.-X. Mechanistic Study on Gold-Catalyzed Cycloisomerization of Dienenynes Involving Aliphatic C-H Functionalization and Inspiration for Developing a New Strategy to Access Polycarbocycles. *J. Am. Chem. Soc.* **2020**, *142*, 2777–2786.
71. Zheng, T.-L.; Liu, S.-Z.; Huo, C.-Y.; Li, J.; Wang, B.-W.; Jin, D.-P.; Cheng, F.; Chen, X.-M.; Zhang, X.-M.; Xu, X.-T.; Wang, S.-H. Au-Catalyzed 1,3-Acyloxy Migration/Cyclization Cascade: A Direct Strategy toward the Synthesis of Functionalized Abietane-Type Diterpenes. *CCS Chem.* **2020**, *2*, 2795–2802.